Phytochemistry 72 (2011) 199–206

Contents lists available at ScienceDirect

Phytochemistry

journal homepage: www.elsevier.com/locate/phytochem

# Detoxification of cruciferous phytoalexins in *Botrytis cinerea*: Spontaneous dimerization of a camalexin metabolite

M. Soledade C. Pedras *, Sajjad Hossain, Ryan B. Snitynsky

*Department of Chemistry, University of Saskatchewan, 110 Science Place, Saskatoon, SK, Canada S7N 5C9*

ARTICLE INFO

*Article history:*
Received 6 September 2010
Received in revised form 3 November 2010
Available online 20 December 2010

*Keywords:*
Brassicaceae
Antifungal
*Botrytis cinerea*
*Botryotinia fuckeliana*
Brassilexin
Brassinin
Camalexin
Crucifer
Cyclobrassinin
Detoxification
Phytoalexin

ABSTRACT

Phytopathogenic fungi are able to overcome plant chemical defenses through detoxification reactions that are enzyme mediated. As a result of such detoxifications, the plant is quickly depleted of its most important antifungal metabolites and can succumb to pathogen attack. Understanding and predicting such detoxification pathways utilized by phytopathogenic fungi could lead to approaches to control plant pathogens. Towards this end, the inhibitory activities and metabolism of the cruciferous phytoalexins camalexin, brassinin, cyclobrassinin, and brassilexin by the phytopathogenic fungus *Botrytis cinerea* Pers. (teleomorph: *Botryotinia fuckeliana*) was investigated. Brassilexin was the most antifungal of the phytoalexins, followed by camalexin, cyclobrassinin and brassinin. Although *B. cinerea* is a species phylogenetically related to the phytopathogenic fungus *Sclerotinia sclerotiorum* (Lib) de Bary, contrary to *S. sclerotiorum*, detoxification of strongly antifungal phytoalexins occurred via either oxidative degradation or hydrolysis but not through glucosylation, suggesting that glucosyl transferases are not involved. A strongly antifungal bisindolylthiadiazole that *B. cinerea* could not detoxify was discovered, which resulted from spontaneous oxidative dimerization of 3-indolethiocarboxamide, a camalexin detoxification product.



## 1. Introduction

The phytopathogenic fungus *Botrytis cinerea* Pers. Fr. (teleomorph B*otryotinia fuckeliana* (de Bary) Whetzel) causes grey mold disease and great yield losses in a very large number of crops, including grapevines (*Vitis vinifera*), tomatoes (*Solanum lycopersicum* L.), cabbage (*Brassica oleraceae* L. cv. Capitata), broccoli (*B. oleraceae* L. cv. Italica), tobacco (*Nicotiana tabacum* L.) and strawberries (*Fragaria* × *ananassa).* Losses are caused in both field-grown and in greenhouse-grown horticultural crops prior to and after harvest. *B. cinerea* is difficult to control due to the numerous strategies it uses to infect diverse plant genera (Williamson et al., 2007). For example, *B. cinerea* produces a variety of phytotoxic metabolites that include oxalic acid, polyketide lactones and sesquiterpenoids, and cell-wall-degrading enzymes, together with other pathogenesis related proteins. In addition, pathogenic isolates of *B. cinerea* detoxify the phytoalexin resveratrol from grapevines and produce an ABC transporter that increases tolerance of the pathogen towards the phytoalexin camalexin (**1**) in *Arabidopsis thaliana* (Choquer et al., 2007). Furthermore, the resistance of tobacco to *B. cinerea* was correlated with the accumulation of the phytoalexin scopoletin and the ability of the mycelium, not the spores, to metabolize scopoletin (El Oirdi et al., 2010). Additional evidence suggests that the pathogen elicits the host to induce programmed cell death as an infection strategy (Williamson et al., 2007).

The number of sequenced genomes from both saprophytic and pathogenic fungal species has been increasing rapidly over the last five years, providing new tools to investigate virulence factors in fungi. The species *B. cinerea* and *Sclerotinia sclerotiorum* (Lib) de Bary are among the first necrotrophic fungi to have their genomes sequenced (the Broad Institute, http://www.broad.mit.edu/annotation/fgi/; the Genoscope, http://www.genoscope.cns.fr/) (Fillinger et al., 2007). Using this knowledge, the cloning, purification and characterization of brassinin glucosyl transferase (SsBGT1), the enzyme from *S. sclerotiorum* involved in brassinin (2) detoxification, were reported recently (Sexton et al., 2009). Alignment of the amino acid sequence of SsBGT1 with glucosyltransferases from other fungal species showed that the closest match was found in *B. cinerea*, which displayed 57% amino acid identity. This sequence similarity was not surprising, particularly considering the close phylogenetic relationship between these species, both from the family Sclerotiniaceae (Hirschhaeuser and Froehlich, 2007).

Phytopathogenic fungi are able to overcome plant chemical defenses (inducible and constitutive) through metabolism and detoxification, utilizing a variety of detoxifying enzymes (Pedras and Ahiahonu, 2005). As a result of such detoxification reactions, the plant is depleted of important antifungal metabolites and in many

* Corresponding author. Tel.: +1 306 966 4772; fax: +1 306 966 4730.
*E-mail address:* s.pedras@usask.ca (M.S.C. Pedras).

0031-9422/$ - see front matter © 2010 Elsevier Ltd. All rights reserved.
doi:10.1016/j.phytochem.2010.11.018

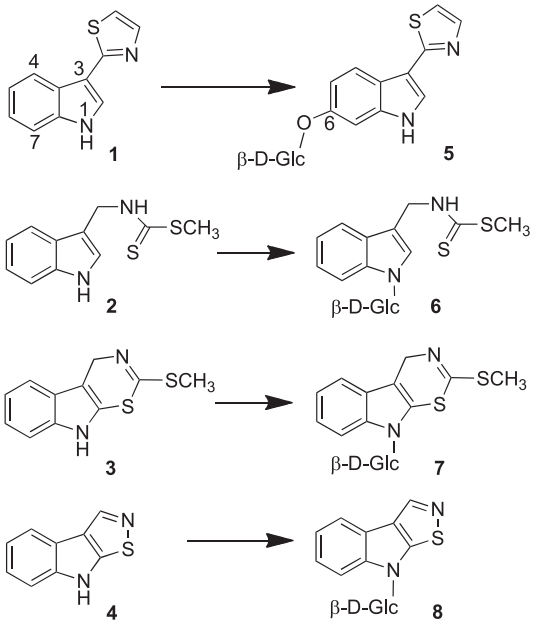


**Fig. 1.** Detoxification pathway of the cruciferous phytoalexins camalexin (**1**), brassinin (**2**), cyclobrassinin (**3**), and brassilexin (**4**) by the phytopathogenic fungus *Sclerotinia sclerotiorum*.

cases succumbs to pathogen attack. Understanding the detoxification pathways utilized by phytopathogenic fungi could lead to new approaches to control plant pathogens. Towards this end, we investigated the metabolism of cruciferous phytoalexins by diverse phytopathogenic fungi, including *S. sclerotiorum* (Pedras and Ahiahonu, 2002; Pedras, 2008). It was established that detoxification of the strongly antifungal phytoalexins camalexin (**1**), brassinin (**2**), cyclobrassinin (**3**), and brassilexin (**4**) involved glucosylation reactions, as summarized in Fig. 1 (Pedras and Ahiahonu, 2002; Pedras et al., 2004; Pedras and Hossain, 2006). In addition, contrary to other phytopathogenic fungi, *S. sclerotiorum* was able to metabolize the strongest antifungal phytoalexin analogues (Pedras and Hossain, 2007).

The economic significance of plant diseases caused by *B. cinerea* and the difficulties in controlling this pathogen using available methodologies (Choquer et al., 2007; Williamson et al., 2007) prompted this investigation. Although it is clear that an ABC transporter is a virulence factor that increases tolerance of the pathogen towards the phytoalexin camalexin (**1**) (*A. thaliana*) (Stefanato et al., 2009), the pathogen produces additional macromolecules likely to contribute to virulence. In this context, it is of great interest to determine if *B. cinerea* is also able to detoxify camalexin or other cruciferous phytoalexins, similar to *S. sclerotiorum* (Pedras and Ahiahonu, 2002). A methodology based on this knowledge to protect plants against *B. cinerea* could be devised (Pedras, 2008). Hence, to compare detoxification pathways of plant defenses in *B. cinerea* and *S. sclerotiorum*, the cruciferous phytoalexins camalexin (**1**), brassinin (**2**), cyclobrassinin (**3**), and brassilexin (**4**) were investigated herein. It was established that the phytoalexins camalexin (**1**) and brassilexin (**4**) displayed the strongest inhibitory activity against *B. cinerea*, but their detoxification reactions were rather different from those occurring in *S. sclerotiorum*.

## 2. Results and discussion

### 2.1. Syntheses and antifungal activity of phytoalexins

The phytoalexins camalexin (**1**), brassinin (**2**), cyclobrassinin (**3**), and brassilexin (**4**) were synthesized and purified as previously reported (Pedras et al., 2007b). Satisfactory spectroscopic data were obtained for all synthetic compounds.

The antifungal activity of each phytoalexin against *B. cinerea* was determined employing the mycelial radial growth assay described in the Experimental, and using $CH_3CN$ or DMSO to dissolve each compound. The results of these assays are shown in Table 1. Brassilexin (**4**) was more inhibitory to *B. cinerea* than camalexin (**1**), brassinin (**2**), or cyclobrassinin (**3**). At 0.10 mM brassilexin (**4**) inhibited completely the growth of *B. cinerea*, while at 0.050 mM the inhibitory effect was slightly lower (89% for UAMH 1784 and 98% for UAMH 1809). Camalexin (**1**) caused complete growth inhibition at 0.20 mM, whereas brassinin (**2**) and cyclobrassinin (**3**) caused complete inhibition at 0.50 mM. At 0.10 mM, the inhibitory effect of camalexin (**1**) was lower than brassilexin (**4**), causing 57% and 54% inhibition for UAMH 1784 and UAMH 1809, respectively. Interestingly, the solvent used to dissolve each phytoalexin affected the activity of each phytoalexin somewhat differently (Table 1). Namely, it was noted that the mycelial growth of the fungus was a regular circle in the presence of DMSO, but the circle was rather irregular in the presence of $CH_3CN$. We attribute these differences partly to the volatility of $CH_3CN$.

Previously, brassilexin (**4**) was shown to inhibit completely the growth of *S. sclerotiorum* at 0.050 mM (Pedras and Hossain, 2006), whereas camalexin (**1**) caused ca. 81% inhibition at similar concentration and brassinin (**2**) was inhibitory only at 0.30 mM (Pedras et al., 2004; Pedras and Hossain, 2007).

### 2.2. Biotransformation of phytoalexins in cultures of B. cinerea

Cultures of *B. cinerea* isolates UAMH 1784 and UAMH 1809 were incubated with each phytoalexin and their transformations were monitored by HPLC (photodiode array and ESI detection). Samples were withdrawn from cultures immediately after addition of each compound and then as described for each case, up to six days. The samples were subjected to neutral, acidic and basic extractions, and the extracts were analyzed by HPLC, as reported in the Experimental. Media incubated with each phytoalexin or metabolites (control solutions) were analyzed similarly to determine the chemical stability of each compound during the incubation experiments.

**Table 1**
Antifungal activity of cruciferous phytoalexins (dissolved in DMSO or $CH_3CN$) against *Botrytis cinerea* isolates UAMH 1784 and UAMH 1809 (27–32 h incubation on agar plates) under continuous light.

| Phytoalexins (mM) | % Inhibition[a] ± standard deviation | | | |
|---|---|---|---|---|
| | UAMH 1784 | | UAMH 1809 | |
| | DMSO | $CH_3CN$ | DMSO | $CH_3CN$ |
| *Camalexin (**1**)* | | | | |
| 0.20 | 100 | 100 | 100 | 100 |
| 0.10 | 57 ± 1 | 38 ± 3 | 54 ± 2 | 38 ± 3 |
| 0.050 | 28 ± 2 | 32 ± 3 | 29 ± 2 | 28 ± 3 |
| *Brassinin (**2**)* | | | | |
| 0.50 | 100 | 100 | 100 | 100 |
| 0.20 | 60 ± 1 | 51 ± 3 | 59 ± 1 | 60 ± 1 |
| 0.10 | 34 ± 1 | 22 ± 2 | 30 ± 2 | 31 ± 4 |
| *Cyclobrassinin (**3**)* | | | | |
| 0.50 | 100 | Not soluble | 100 | Not soluble |
| 0.20 | 70 ± 7 | 74 ± 7 | 66 ± 10 | 70 ± 10 |
| 0.10 | 24 ± 5 | 36 ± 4 | 41 ± 13 | 39 ± 8 |
| *Brassilexin (**4**)* | | | | |
| 0.10 | 100 | 100 | 100 | 100 |
| 0.050 | 89 ± 2 | 88 ± 2 | 98 ± 4 | 99 ± 3 |
| 0.025 | 54 ± 2 | 66 ± 5 | 83 ± 11 | 80 ± 9 |

[a] Percentage of growth inhibition calculated using the formula: % inhibition = 100 − [(growth on amended/growth in control) × 100]; values represent the mean and standard deviation of at least two independent experiments conducted in triplicate.

*2.2.1. Camalexin (**1**)*

The HPLC chromatograms of neutral extracts of cultures of isolates UAMH 1784 and UAMH 1809 incubated with camalexin (**1**) showed that it was almost completely metabolized within 12 h (Fig. 2). The chromatograms of neutral extracts showed the presence of camalexin (**1**) and additional peaks that were due to 3-indolecarboxynitrile (**10**, $t_R$ = 7.8 ± 0.2 min) and 3-indolecarboxylic acid (**11**, $t_R$ = 3.6 ± 0.1 min), by comparison with authentic samples; additional peaks at $t_R$ = 4.6 and $t_R$ = 20.5 min could not be readily identified. Isolation of these metabolites from larger scale cultures, as described in the Experimental, and analyses of spectroscopic data allowed the identification of the peak with $t_R$ = 4.6 min as 3-indolethiocarboxamide (**9**) (Fig. 3). Due to the small amounts obtained, the structure of the metabolite with $t_R$ = 20.5 min was only tentatively assigned as the bisindolylthiadiazole **12**, a hitherto unknown compound. None of these metabolites were detected either in control cultures or in media incubated with camalexin (**1**). No other metabolites were detected in either the acidic or basic extracts of either culture. Furthermore, the rate of camalexin (**1**) transformation was not light dependent.

To establish the sequence of steps of camalexin (**1**) transformation, the thiocarboxamide **9** was prepared as described in the Experimental and administered separately to cultures of isolates UAMH 1784 and UAMH 1809. The cultures were incubated, extracted and analyzed as described in the Experimental. As expected, indole-3-thiocarboxamide (**9**) was transformed to the nitrile **10**, which in turn was slowly (more than four days) transformed to 3-indolecarboxylic acid (**11**) (Fig. 3). Control solutions of medium containing thiocarboxamide **9** indicated that it was not stable, as small amounts of the nitrile **10** and bisindolylthiadiazole **12** were detected in medium extracts after 6 h. Nonetheless, the transformation of 3-indolethiocarboxamide (**9**) in fungal cultures ($T_{1/2}$ = 10 h and 18 h, Fig. 4) was much faster than in control medium solutions ($T_{1/2}$ = 36 h, Fig. 4), indicating that this transformation was enzyme mediated. Formation of the bisindolylthiadiazole **12** did not occur in aqueous solutions or in aqueous acetonitrile, thus it is likely that medium components caused the oxidative dimerization of thiocarboxamide **9** to **12**.

A literature search indicated that 3,5-bisphenyl-1,2,4-thiadiazoles could be synthesized from IBX (*o*-iodoxybenzoic acid) mediated oxidative dimerization of thioamides (Patil et al., 2009). Hence, application of this methodology to 3-indolethiocarboxamide (**9**) yielded **12** in reasonable yield, as described in the Experimental and summarized in Fig. 5. 3,5-(3′,3″-Bisindolyl)-1,2,4-thiadiazole (**12**) was administered to cultures of isolates UAMH 1784 and UAMH 1809 and cultures analyzed over a four-day period. HPLC chromatograms indicated that thiadiazole **12** was not metabolized by *B. cinerea*.

The antifungal activity of the metabolites of camalexin (**1**) to isolates UAMH 1784 and UAMH 1809 of *B. cinerea* were determined employing the mycelial radial growth assay described in Section 2 and using DMSO to dissolve each compound. The results of these assays are shown in Table 2. Metabolites **9**–**11** were substantially less inhibitory to isolates UAMH 1784 and UAMH 1809 than camalexin (**1**) itself, indicating that both isolates detoxify camalexin efficiently. 3,5-(3′,3″-Bisindolyl)-1,2,4-thiadiazole (**12**)

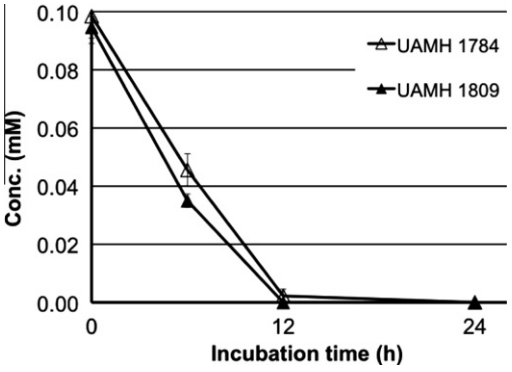


**Fig. 2.** Progress curves for transformation of the phytoalexin camalexin (**1**, 0.10 mM) by *Botrytis cinerea* isolates UAMH 1784 and UAMH 1809. Concentrations were determined using calibration curves; each point is the average of at least three independent experiments ± standard deviation.

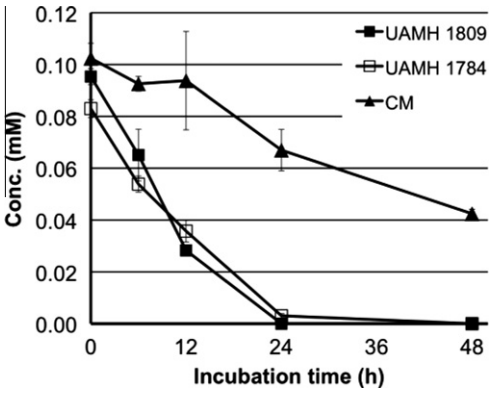


**Fig. 4.** Progress curves for transformation of 3-indolethiocarboxamide (**9**, 0.10 mM) by *Botrytis cinerea* isolates UAMH 1784 and UAMH 1809, and in control medium (CM). Concentrations were determined using calibration curves; each point is the average of at least three independent experiments ± standard deviation.

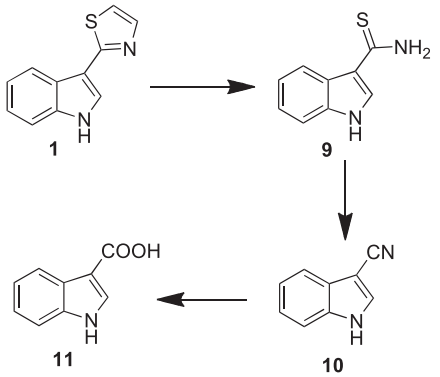


**Fig. 3.** Transformation pathway of the phytoalexin camalexin (**1**) by *Botrytis cinerea* isolates UAMH 1784 and UAMH 1809.

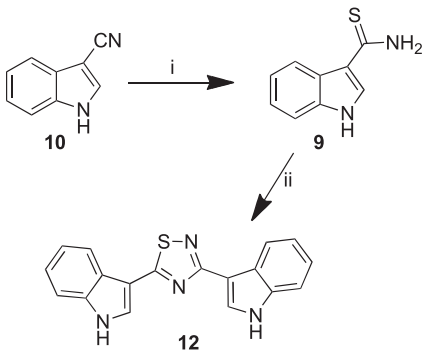


**Fig. 5.** Synthesis of 3-indolethiocarboxamide (**9**) and 3,5-(3′,3″-bisindolyl)-1,2,4-thiadiazole (**12**). Reagents and conditions: (i) $CH_3CSNH_2$, HCl/DMF, reflux; (ii) IBX (*o*-iodoxybenzoic acid), $CH_3CN$, r.t.

**Table 2**
Antifungal activity of camalexin metabolites **9**–**11** and 3,5-(3′,3″-bisindolyl)-1,2,4-thiadiazole (**12**) (dissolved in DMSO) against *Botrytis cinerea* isolates UAMH 1784 and UAMH 1809 (27–32 h incubation on agar plates) under continuous light.

| Compound (mM) | % Inhibition[a] ± standard deviation | |
|---|---|---|
| | UAMH 1784 | UAMH 1809 |
| *3-Indolethiocarboxamide (**9**)* | | |
| 0.50 | 64 ± 2 | 68 ± 2 |
| 0.20 | 48 ± 2 | 45 ± 2 |
| 0.10 | 32 ± 2 | 21 ± 2 |
| *3-Indolecarboxynitrile (**10**)* | | |
| 0.50 | 65 ± 2 | 60 ± 2 |
| 0.20 | 34 ± 2 | 37 ± 2 |
| 0.10 | 24 ± 2 | 11 ± 1 |
| *3-Indolecarboxylic acid (**11**)* | | |
| 0.50 | 31 ± 2 | 27 ± 2 |
| 0.20 | 14 ± 2 | 14 ± 2 |
| 0.10 | 6 ± 2 | 7 ± 1 |
| *3,5-(3′,3″-Bisindolyl)-1,2,4-thiadiazole (**12**)* | | |
| 0.50 | Not soluble | Not soluble |
| 0.20 | 76 ± 2 | 75 ± 1 |
| 0.10 | 68 ± 2 | 71 ± 2 |
| 0.05 | 49 ± 2 | 38 ± 2 |

[a] Percentage of growth inhibition calculated using the formula: % inhibition = 100 − [(growth on amended/growth in control) × 100]; values represent the mean and standard deviation of two independent experiments conducted in triplicate.

was more inhibitory to isolates UAMH 1784 and UAMH 1809 than any of the camalexin metabolites, but less inhibitory than camalexin (**1**) (ca. 76% for **12** vs. 100% for **1**).

It is noteworthy that a few bis(indole)alkaloids from marine organisms, such as the nortopsentins A–C, containing a 2,4-bis (3-indolyl)imidazole skeleton, exhibit antibacterial, antiviral and cytotoxic activities. The imidazole moiety of the nortopsentins was replaced with a thiazole, pyrazinone or pyrazine moiety to yield bis(indolyl) alkaloids displaying anti-tumor activity (Jiang and Gu, 2000). In addition, the synthesis of 3,5-disubstituted-1,2,4-oxadiazoles containing indolyl moieties was also described (Shvekhgeimer et al., 1984), but to date no 3,5-(3′,3″-bisindolyl)-1,2,4-thiadiazoles have been reported.

Previous work showed that camalexin (**1**) was detoxified by the phytopathogenic fungus *Rhizoctonia solani* Kuhn to 5-hydroxycamalexin (**13**), which was further transformed into metabolites **14** and **15** (Fig. 6), substantially less inhibitory to the pathogen than camalexin (**1**) (Pedras and Khan, 2000). Interestingly camalexin transformation to 5-hydroxycamalexin (**13**) was much faster under light conditions (ca. 24 h in light vs. 8–10 days in dark); however, light did not affect the biotransformation rates of camalexin (**1**) in cultures of *B. cinerea*. *S. sclerotiorum* detoxified camalexin (**1**) through oxidation to the corresponding 6-hydroxy derivative followed by glucosylation to yield 6-(*O*-*β*-D-glucopyranosyl)camalexin (**5**) (Pedras and Ahiahonu, 2002). On the other hand, some plant pathogenic fungi and bacteria did not transform camalexin (**1**), including many isolate types of *Leptosphaeria maculans* and *Alternaria brassicae* (Pedras et al., 1998).

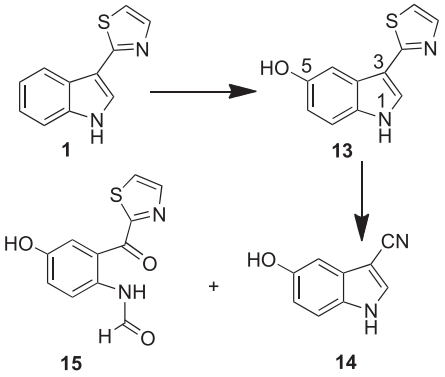


**Fig. 6.** Transformation pathway of the phytoalexin camalexin (**1**) by *Rhizoctonia solani* virulent isolate AG 2-1.

*2.2.2. Brassinin (**2**)*

Analyses of HPLC chromatograms of neutral extracts of cultures of isolates UAMH 1784 and UAMH 1809 incubated with brassinin (**2**) showed that it was almost completely metabolized within 24 h (Fig. 7). Furthermore, the chromatograms of neutral extracts showed the presence of additional peaks that were due to *N*′-acetyl-3-indolylmethanamine (**17**, $t_R$ = 4.4 ± 0.2 min) and 3-indolecarboxylic acid (**11**) by comparison with authentic samples (Fig. 8). The acidic extracts showed traces of brassinin (**2**) plus **11** and the basic extracts indicated the presence of 3-indolylmethanamine (**16**). None of these metabolites were detected either in control cultures or in medium incubated with brassinin (**2**). HPLC detection and quantification of amine 16% in basic extracts was carried out using HPLC method B. Further analysis of the HPLC chromatograms of the transformation of brassinin (**2**) showed that both amine **16** and acetyl amine **17** remained in cultures for more than four days.

To establish the sequence of steps of brassinin (**2**) transformation, amine **16** was administered to cultures of isolates UAMH 1784 and UAMH 1809, and cultures were incubated and analyzed as described above. The HPLC chromatograms of culture extracts indicated that amine **16** was slowly transformed to acetyl amine **17** (more than four days), 3-indolecarboxaldehyde (**18**) and 3-indolecarboxylic acid (**11**). Antifungal bioassays showed that the metabolites of brassinin (**2**) were substantially less inhibitory to isolates UAMH 1784 and UAMH 1809 than brassinin itself (Table 3), indicating that both isolates detoxify brassinin (**2**).

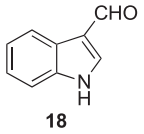


The transformation pathway of brassinin (**2**) by *B. cinerea* was similar to the pathways previously observed for *L. maculans* isolates Laird 2/Mayfair 2 (Pedras et al., 2007a), *L. biglobosa* (Pedras

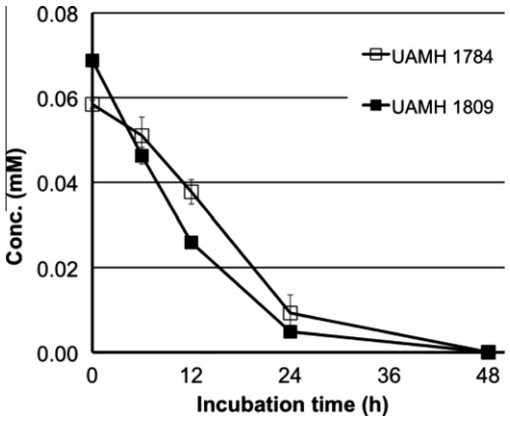


**Fig. 7.** Progress curves for transformation of the phytoalexin brassinin (**2**, 0.10 mM) by *Botrytis cinerea* isolates UAMH 1784 and UAMH 1809. Concentrations were determined using calibration curves; each point is the average of at least three independent experiments ± standard deviation.

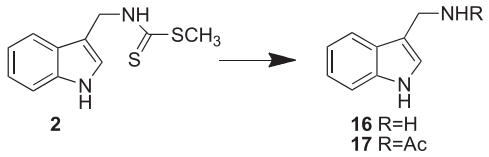


**Fig. 8.** Transformation pathway of the phytoalexin brassinin (**2**) by *Botrytis cinerea* isolates UAMH 1784 and UAMH 1809.

**Table 3**
Antifungal activity of brassinin metabolites **16** and **17** (dissolved in DMSO) against *Botrytis cinerea* isolates UAMH 1784 and UAMH 1809 (27–32 h incubation on agar plates) under continuous light.

| Compound (mM) | % Inhibition[a] ± standard deviation | |
|---|---|---|
| | UAMH 1784 | UAMH 1809 |
| *3-Indolylmethanamine (**16**)* | | |
| 0.50 | 26 ± 3 | 38 ± 2 |
| 0.20 | 19 ± 3 | 15 ± 0 |
| 0.10 | 14 ± 3 | 15 ± 4 |
| *$N_b$-Acetyl-3-indolylmethanamine (**17**)* | | |
| 0.50 | 38 ± 2 | 30 ± 2 |
| 0.20 | 22 ± 2 | 21 ± 2 |
| 0.10 | 16 ± 2 | 11 ± 2 |

[a] Percentage of growth inhibition calculated using the formula: % inhibition = 100 − [(growth on amended/growth in control) × 100]; values represent the mean and standard deviation of at least two independent experiments conducted in triplicate.

and Taylor, 1993) and *A. brassicicola* (Pedras et al., 2009). Despite the sequence similarity between the brassinin detoxifying glucosyl transferase from *S. sclerotiorum* (SsBGT1) and the putative protein present in *B. cinerea* (BC1G_07249, 57% amino acid identity), no traces of 1-*β*-D-glucopyranosylbrassinin (**6**) were detected in cultures of any of the isolates of *B. cinerea* incubated with brassinin (**2**).

### 2.2.3. Cyclobrassinin (*3*) and brassilexin (*4*)

Analyses of HPLC chromatograms of neutral extracts of cultures of isolates UAMH 1784 and UAMH 1809 incubated with cyclobrassinin (**3**) showed that it was almost completely metabolized within 12 h (Fig. 9). The chromatograms of neutral extracts showed the presence of additional peaks that were due to cyclobrassinin sulfoxide (**19**, $t_R$ = 11.8 ± 0.1 min), and brassilexin (**4**, $t_R$ = 9.4 ± 0.2 min), by direct comparison with authentic samples. No

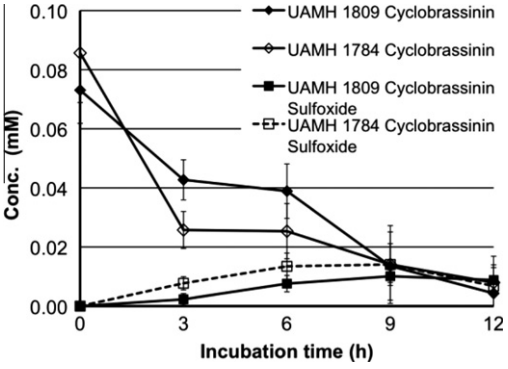


**Fig. 9.** Progress curves for transformation of the phytoalexin cyclobrassinin (**3**, 0.10 mM) by *Botrytis cinerea* isolates UAMH 1784 and UAMH 1809 and formation of cyclobrassinin sulfoxide (**19**). Concentrations were determined using calibration curves; each point is the average of at least three independent experiments ± standard deviation.

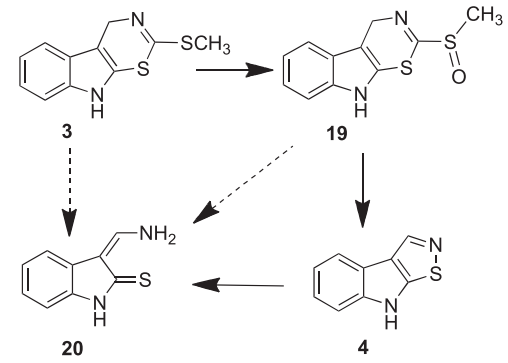


**Fig. 10.** Transformation pathways of the phytoalexins cyclobrassinin (**3**) and brassilexin (**4**) by *Botrytis cinerea* isolates UAMH 1784 and UAMH 1809. Dashed arrows represent potential transformation.

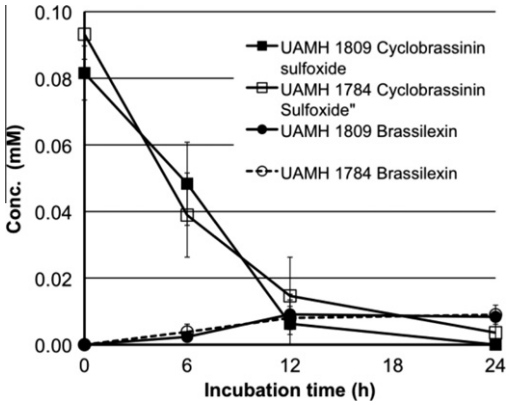


**Fig. 11.** Progress curves for transformation of the phytoalexin cyclobrassinin sulfoxide (**19**, 0.10 mM) by *Botrytis cinerea* isolates UAMH 1784 and UAMH 1809 and formation of brassilexin (**4**). Concentrations were determined using calibration curves; each point is the average of at least three independent experiments ± standard deviation.

additional metabolites were detected in the acidic or basic culture extracts. Cultures of isolates UAMH 1784 and UAMH 1809 were also incubated with cyclobrassinin sulfoxide (**19**), extracted and analyzed by HPLC. Results of these experiments indicated that cyclobrassinin sulfoxide (**19**) was transformed into brassilexin (**4**) (Fig. 10). However, it is not clear whether transformation of cyclobrassinin occurs always via **19** or both transformations occur, i.e. **3** can also give directly **4** (Figs. 10 and 11). Ultimately, purification of the enzyme(s) catalyzing these transformations will clarify the situation.

Although cyclobrassinin (**3**) was previously reported to decompose to undetermined compounds upon treatment with MCPBA (Devys et al., 1990), in our hands, its oxidation using MCPBA afforded sulfoxide **19** in 27% yield, as described in the Experimental. By contrast, oxidation of cyclobrassinin (**3**) using periodate was reported to yield brassilexin (**4**) (Devys and Barbier, 1992). Cyclobrassinin sulfoxide (**19**) was previously described as a phytoalexin of *B. juncea* (Devys et al., 1990), however complete NMR spectroscopic characterization is reported here for the first time. Cyclobrassinin sulfoxide (**19**) was more inhibitory to *B. cinerea* than cyclobrassinin (**3**).

Analyses of HPLC chromatograms of neutral extracts of cultures incubated with brassilexin (**4**) at 0.05 mM (due to higher toxicity lower conc. was used) indicated that it was almost completely metabolized within two days (Fig. 12). Furthermore, the chromatograms of neutral extracts indicated the presence of a peak identified as 3-aminomethyleneindole-2-thione (20, $t_R$ = 4.9 ± 0.2 min).

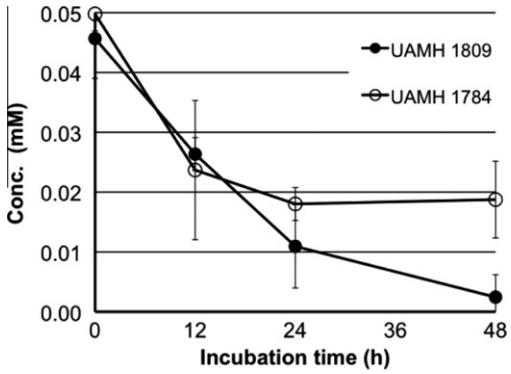


**Fig. 12.** Progress curves for transformation of the phytoalexin brassilexin (**4**, 0.05 mM) by *Botrytis cinerea* isolates UAMH 1784 and UAMH 1809. Concentrations were determined using calibration curves; each point is the average of at least three independent experiments ± standard deviation.

This metabolite was further transformed enzymatically to metabolites not extractable with EtOAc, likely due to their higher solubility in aqueous media. None of these metabolite(s) were detected either in control cultures or in medium incubated with cyclobrassinin (**3**) or brassilexin (**4**). Aminomethyleneindole-2-thione (**20**) oxidized spontaneously to brassilexin (**4**) at much slower rate than its enzymatic reduction, as previously established (Pedras and Suchy, 2005). Due to its lower stability, solutions of **20** were obtained containing some brassilexin and thus **20** was not tested for inhibitory activity against isolates UAMH 1784 and UAMH 1809. The complete transformations of cyclobrassinin (**3**) and brassilexin (**4**) by isolates UAMH 1784 and UAMH 1809 led to metabolites that did not inhibit mycelial growth.

Previously, cyclobrassinin (**3**) was found to be converted to the phytoalexin dioxibrassinin (**21**) and further to non-toxic undetermined metabolites by isolates of *L. maculans* virulent on canola (Pedras and Ahiahonu, 2005), whereas *L. maculans* isolates Laird 2/Mayfair 2 transformed cyclobrassinin (**3**) to 3-aminomethyleneindole-2-thione (**20**) and to other polar and non-antifungal metabolites (Pedras and Snitynsky, 2010). Considering that **20** was not detected in cultures incubated with cyclobrassinin (**3**) during the first 12 h, it is not clear whether this metabolite was formed directly from cyclobrassinin (**3**) or if it resulted only from brassilexin (**4**). Similarly, brassilexin (**4**) was converted by various isolate types of *L. maculans* to 3-aminomethyleneindole-2-thione (**20**) and to other polar and non-antifungal metabolites (Pedras and Suchy, 2005). It is noteworthy that *S. sclerotiorum* remains unique in its glucosylation of the most antifungal cruciferous phytoalexins (Pedras and Hossain, 2006).

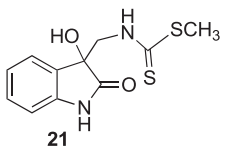


**21**

## 3. Conclusion

Altogether our results suggest that phytoalexin detoxification may contribute to the virulence of *B. cinerea* in crucifers. Furthermore, our results demonstrate the importance of considering detoxification of phytoalexins in plants infected with *B. cinerea*, before drawing conclusions based on the amounts of phytoalexins produced. For example, metabolic studies in the interaction of *B. cinerea* with *A. thaliana* have to consider that camalexin (**1**) is detoxified to products that could be presumed as plant products (e.g. **9**), but actually result from fungal metabolism. It is surmised that detoxification reactions of phytoalexins carried out by phytopathogenic fungi do not appear to be predictable, even when there is a substantial sequence similarity between a detoxifying enzyme from one species and a putative protein from a phylogenetically related species. Indeed, *S. sclerotiorum* was previously shown to glucosylate brassinin (**2**) using SsBGT1, but no evidence of such transformation was found in this study with *B. cinerea*, which produces a putative protein showing 57% amino acid identity to SsBGT1, (Accession No. BC1G_07249, Sexton et al., 2009). *S. sclerotiorum* was previously shown to also glucosylate the phytoalexins camalexin (**1**), cyclobrassinin (**3**) and brassilexin (**4**), but *B. cinerea* did not carry out similar transformations under our experimental conditions.

## 4. Experimental

### 4.1. Chemicals and instrumentation

All chemicals were purchased from Sigma–Aldrich Canada Ltd., Oakville, ON; solvents were HPLC grade and used as such. Organic extracts were dried with $Na_2SO_4$ and solvents removed under reduced pressure using a rotary evaporator. Flash column chromatography (FCC) was carried out using silica gel grade 60, mesh size 230–400 Å. Preparative thin layer chromatography (prep TLC) was carried out on silica gel plates, Kieselgel 60 $F_{254}$.

Nuclear magnetic resonance (NMR) spectra were recorded on Bruker 500 MHz Avance spectrometers, for $^1H$, 500.3 MHz and for $^{13}C$, 125.8 MHz; chemical shifts ($\delta$) are reported in parts per million (ppm) relative to TMS; spectra were calibrated using the solvent peaks; spin coupling constants ($J$) are reported to the nearest 0.5 Hz. Fourier transform infrared (FT-IR) data were recorded on a spectrometer and spectra were measured by the diffuse reflectance method on samples dispersed in KBr. MS [high resolution (HR), electron impact (EI)] were obtained on a VG 70 SE mass spectrometer employing a solids probe.

HPLC analysis was carried out with Agilent high performance liquid chromatography instruments equipped with quaternary pump, automatic injector, and diode array detector (DAD, wavelength range 190–600 nm), degasser, and a column, having an in-line filter. Method A: column Eclipse XDB-C18 (5 μm particle size silica, 4.6 i.d. × 150 mm), mobile phase $H_2O$–MeOH (1:1, v/v) to MeOH, for 25.0 min, linear gradient, and at a flow rate 0.75 ml/min; method B (for amines both solvents containing 0.01% propanamine): Zorbax ODS (3.5 μm particle size silica, 3.0 i.d. × 100 mm), mobile phase $H_2O$–MeOH (1:9, v/v) to MeOH, for 5.0 min, linear gradient, MeOH, for 15.0 min, at a flow rate of 0.50 ml/min. HPLC–DAD-ESI-MS analysis were carried out with an Agilent 1100 series HPLC system equipped with an autosampler, binary pump, degasser, and a diode array detector connected directly to a mass detector (Agilent G2440A MSD-Trap-XCT ion trap mass spectrometer) with an electrospray ionization (ESI) source. Chromatographic separation was carried out at room temperature using an Eclipse XDB C-18 column (5 μm particle size silica, 4.6 i.d. × 150 mm). The mobile phase consisted of a linear gradient of 0.2% $HCO_2H$ in $H_2O$ and 0.2% $HCO_2H$ in $CH_3CN$ (75:25 to 25:75 in 35 min, to 0:100 in 5 min) and a flow rate of 1 ml/min. Data acquisition was carried out in positive and negative polarity modes in a single LC run. Data processing was carried out with Agilent Chemstation Software. HPLC–HR-ESI-MS was performed on an Agilent HPLC 1100 series directly connected to a QSTAR XL Systems Mass Spectrometer (Hybrid Quadrupole-TOF LC/MS/MS) with turbo spray ESI source. Chromatographic separation was carried out

at room temperature using a Hypersil ODS C-18 column (5 μm particle size silica, 2.1 i.d. × 200 mm) or a Hypersil ODS C-18 column (5 μm particle size silica, 2.1 i.d. × 100 mm). The mobile phase consisted of a linear gradient of 0.1% $HCO_2H$ in $H_2O$ and 0.1% $HCO_2H$ in $CH_3CN$ (75:25 to 25:75 in 35 min, to 0:100 in 5 min) and a flow rate of 0.25 ml/min. Data processing was carried out by Analyst QS Software.

### 4.2. Mycelial radial growth assays

*B. cinerea* isolates UAMH 1784 and UAMH 1809 isolated from soft rot on plum and dogwood leaf, respectively, were obtained from the University of Alberta Microfungus Collection and Herbarium.

Spores were spotted onto potato dextrose agar plates (PDA) and allowed to grow for three days under constant light at 23 ± 1 °C. Plugs (4 mm) were cut from the edges of the mycelia and placed inverted onto six-well plates containing phytoalexins in either DMSO or $CH_3CN$ mixed into potato dextrose agar. The final concentrations of each phytoalexin in agar varied from 0.02 to 0.50 mM, with a DMSO or $CH_3CN$ concentration of 1%. The plates were allowed to grow under constant light at 23 ± 1 °C up to 48 h; the diameter of the mycelial mat was measured and compared to control mycelia grown on plates containing DMSO or $CH_3CN$ only.

### 4.3. Liquid fungal cultures and biotransformation studies

Liquid cultures of were grown in 250 ml Erlenmeyer flasks containing 100 ml of minimal medium inoculated fungal spores for a final concentration of $1 \times 10^4$/100 ml, or six mycelial plugs (6 mm diameter) per 100 ml, and cultures were incubated on a shaker at 120 rpm. After 48–72 h at 23 ± 1 °C (96 h for cyclobrassinin sulfoxide), under constant light, a solution of the phytoalexin or compound in $CH_3CN$ (100–250 μl) was added to the cultures, for a final concentration of 0.10 mM, except brassilexin (**4**) that was 0.050 mM. The flasks were returned to the shaker, and samples (5 ml) were withdrawn at various times and either extracted immediately with EtOAc or immediately frozen. The EtOAc residue was dissolved in MeOH or $CH_3CN$ and analyzed by HPLC, as described above.

### 4.4. Syntheses of 3-indolethiocarboxamide (*9*) and 3,5-(3′,3″-bisindolyl)-1,2,4-thiadiazole (*12*)

3-Indolethiocarboxamide (**9**) was prepared from 3-indolecarboxynitrile (**10**) by modification of a previously published procedure (Gu et al., 1999), as follows. A mixture of 3-indolecarboxynitrile (100 mg, 0.700 mmol) and thioacetamide (105 mg, 1.40 mmol) in 10% HCl–DMF solution (1.5 ml) was stirred at 95 °C for 12 h. The reaction mixture was then neutralized with $NaHCO_3$ (sat. solution), extracted with EtOAc, the organic layer was dried and separated by FCC (silica gel, $CH_2Cl_2$–MeOH, 99:1) to afford indole-3-thiocarboxamide (**9**) (71.5 mg, 59%). The $^{13}C$ NMR spectroscopic data of **9** is reported here for the first time, other spectroscopic data being similar to that previously reported (Jiang and Gu, 2000).

#### 4.4.1. 3-Indolethiocarboxamide (*9*)

HPLC $t_R$ = 4.6 min (method A). $^1H$ NMR (DMSO-$d_6$) $\delta$ 10.91 (1H, s), 8.08 (1H, s), 7.95 (1H, s), 7.75 (1H, d, $J$ = 7.5 Hz), 7.22 (1H, d, $J$ = 3 Hz), 6.56 (1H, d, $J$ = 8 Hz), 6.29 (1H, dd, $J$ = 7, 7 Hz), 6.26 (1H, dd, $J$ = 7, 7 Hz). $^{13}C$ NMR (DMSO-$d_6$) $\delta$ 193.6, 136.8, 128.1, 125.9, 122.0, 121.8, 120.7, 116.3, 112.0. HREI-MS *m/z*: calc. for $C_9H_8N_2S_2$ 176.0409, found 176.0408; *m/z* (%):176.0 $[M]^+$ (100), 160.0 (24), 143.1 (84), 142.1 (43), 116.0 (20). UV (HPLC, $CH_3OH$–$H_2O$) $\lambda_{max}$ (nm): 215, 255, 318. FTIR (KBr, $cm^{-1}$) $\nu_{max}$: 3190, 1621, 1527, 1442, 850.

3-Indolethiocarboxamide (**9**) (100 mg, 0.570 mmol) was added to a stirred suspension of IBX (166 mg, 0.630 mmol) in $CH_3CN$ (2.0 ml). After completion of the reaction, the residue was filtered off and the solvent was evaporated under reduced pressure. The reaction mixture residue was dissolved in EtOAc (20 ml), washed with $NaHCO_3$ (sat. solution) and then $H_2O$. The organic layer was dried and concentrated under reduced pressure, and the residue was fractionated by FCC (silica gel, $CH_2Cl_2$–MeOH, 99:1) to yield 3,5-(3′,3″-bisindolyl)-1,2,4-thiadiazole (**12**) (40.5 mg, 45%) and 3-indolecarboxynitrile (**10**) (16.1 mg, 20%).

#### 4.4.2. 3,5-(3′,3″-Bisindolyl)-1,2,4-thiadiazole (*12*)

HPLC $t_R$ = 20.5 min (method A). $^1H$ NMR $\delta$ (500 MHz, DMSO-$d_6$) 11.26 (1 H, s), 10.85 (1H, s), 7.61 (1H, m), 7.55 (1H, m), 6.71–6.65 (2H, m), 6.48–6.43 (2H, m), 6.38–6.34 (2H, m). $^{13}C$ NMR $\delta$ (125.8 MHz, DMSO-$d_6$) 180.2, 169.7, 136.7, 136.6, 129.3, 128.7, 125.1, 124.3, 122.8, 122.1, 121.5, 121.1, 121.5, 120.2, 112.0, 111.2, 110.2, 107.6. HREI-MS *m/z*: calc. for $C_{18}H_{12}N_4S$: 316.0787, found 316.0783; *m/z* (%): 316.0 $[M]^+$ (81), 200.0 (19), 174.0 (100), 142.1 (57), 115.0 (18). UV (HPLC, $CH_3OH$–$H_2O$) $\lambda_{max}$ (nm): 220, 253, 318. FTIR (KBr, $cm^{-1}$) $\nu_{max}$: 3100, 1531, 1338, 1236, 744.

### 4.5. Synthesis of cyclobrassinin sulfoxide (*19*)

*m*-Chloroperoxybenzoic acid (MCPBA, 30 mg, 0.17 mmol) in MeOH (1.5 ml) was added to a solution of cyclobrassinin (**3**, 20 mg, 0.085 mmol) in MeOH (1 ml) at room temperature, and the reaction mixture was stirred for 30 min. The reaction mixture was cooled to 0 °C, dimethylsulfide was added (200 ml to destroy MCPBA) and the reaction was stirred for another 30 min. The solvent was evaporated under reduced pressure, the residue was dissolved in EtOAc (4 ml), the solution was washed with $Na_2CO_3$, dried over $Na_2SO_4$, and concentrated to yield the crude product. The purified product was obtained after FCC (silica gel, hexane–EtOAc, 2:1) to yield cyclobrassinin sulfoxide (**19**, 5.7 mg, 27% yield). HPLC $t_R$ = 10.5 min (method A). $^1H$ NMR ($CD_2Cl_2$): $\delta$ 8.75 (br s, 1H), 7.45 (d, $J$ = 7.5 Hz, 1H), 7.39 (d, $J$ = 7.5 Hz, 1H), 7.19 (dd, $J$ = 7.5, 7.5 Hz, 1H), 7.14 (dd, $J$ = 7.5, 7.5 Hz, 1H), 5.42 (s, 2H), 2.86 (s, 3H). $^{13}C$ NMR ($CD_2Cl_2$): $\delta$ 166.5, 137.4, 125.0, 122.9, 121.5, 120.9, 117.9, 111.4, 100.4, 50.7, 42.0. HREI-MS *m/z* (%): calc. for $C_{11}H_{10}N_2OS_2$: 250.0234, found 250.0237 (26), 161.0 (100). MS-ESI *m/z* (%): 273 $[M+Na]^+$ (15), 251 (3), 187 (100).

## Acknowledgements

Financial support was obtained from the Natural Sciences and Engineering Research Council of Canada (Discovery Grant to M.S.C.P.), the Canada Research Chairs program, Canada Foundation for Innovation, the Saskatchewan Government, and the University of Saskatchewan (graduate assistantship to S.H.). We acknowledge the technical assistance of K. Brown (NMR), P.B. Chumala (HPLC) and K. Thoms (MS), from the Department of Chemistry.

## Appendix A. Supplementary data

Supplementary data associated with this article (NMR spectra for new compounds **9** and **12** and cyclobrassinin sulfoxide (**19**)) can be found, in the online version, at doi:10.1016/j.phytochem.2010.11.018.

## References

Choquer, M., Fournier, E., Kunz, C., Levis, C., Pradier, J.-M., Simon, A., Viaud, M., 2007. *Botrytis cinerea* virulence factors: new insights into a necrotrophic and polyphageous pathogen. FEMS Microbiology Letters 277, 1–10.

Devys, M., Barbier, M., 1992. In vitro demonstration of a biosynthetic sequence for the *Cruciferae phytoalexins*. Zeitschrift fuer Naturforschung C: Journal of Biosciences 47, 318–319.

Devys, M., Barbier, M., Kollmann, A., Rouxel, T., Bousquet, J.F., 1990. Cyclobrassinin sulfoxide, a sulfur-containing phytoalexin from *Brassica juncea*. Phytochemistry 29, 1087–1088.

El Oirdi, M., Trapani, A., Bouarab, K., 2010. The nature of tobacco resistance against *Botrytis cinerea* depends on the infection structures of the pathogen. Environmental Microbiology 12, 239–253.

Fillinger, S., Amselem, J., Artiguenave, F., 2007. The genome projects of the plant pathogenic fungi *Botrytis cinerea* and *Sclerotinia sclerotiorum*. In: Jeandet, P., Clément, C., Conreux A. (Eds.), Macromolecules of Grape and Wines. Editions TEC and DOC, Paris, France, pp. 125–133.

Gu, X.H., Wan, X.Z., Jiang, B., 1999. Syntheses and biological activities of bis(3-indolyl)thiazoles, analogues of marine bis(indole)alkaloid nortopsentins. Bioorganic and Medicinal Chemistry Letters 9, 569–572.

Hirschhaeuser, S., Froehlich, J., 2007. Multiplex PCR for species discrimination of Sclerotiniaceae by novel laccase introns. International Journal of Food Microbiology 118, 151–157.

Jiang, B., Gu, X.-H., 2000. Syntheses and cytotoxicity evaluation of bis(indolyl) thiazole, bis(indolyl)pyrazinone and bis(indolyl)pyrazine: analogues of cytotoxic marine bis(indole) alkaloid. Bioorganic and Medicinal Chemistry 8, 363–371.

Patil, P.C., Bhalerao, D.S., Dangate, P.S., Akamanchi, K.G., 2009. IBX/TEAB-mediated oxidative dimerization of thioamides: synthesis of 3,5-disubstituted 1,2,4-thiadiazoles. Tetrahedron Letters 50, 5820–5822.

Pedras, M.S.C., 2008. The chemical ecology of crucifers and their fungal pathogens: boosting plant defenses and inhibiting pathogen invasion. The Chemical Record 8, 109–115.

Pedras, M.S.C., Ahiahonu, P.W.K., 2002. Probing the phytopathogenic stem rot fungus with phytoalexins and analogs: unprecedented glucosylation of camalexin and 6-methoxycamalexin. Bioorganic and Medicinal Chemistry 10, 3307–3312.

Pedras, M.S.C., Ahiahonu, P.W.K., 2005. Metabolism and detoxification of phytoalexins and analogs by phytopathogenic fungi. Phytochemistry 66, 391–411.

Pedras, M.S.C., Hossain, M., 2006. Metabolism of crucifer phytoalexins in *Sclerotinia sclerotiorum*: detoxification of strongly antifungal compounds involves glucosylation. Organic and Biomolecular Chemistry 4, 2581–2590.

Pedras, M.S.C., Hossain, M., 2007. Design, synthesis, and evaluation of potential inhibitors of brassinin glucosyl transferase, a phytoalexin detoxifying enzyme from *Sclerotinia sclerotiorum*. Bioorganic and Medicinal Chemistry 15, 5981–5996.

Pedras, M.S.C., Khan, A.Q., 2000. Biotransformation of the phytoalexin camalexin by the root phytopathogen *Rhizoctonia solani*. Phytochemistry 53, 59–69.

Pedras, M.S.C., Snitynsky, R.B., 2010. Impact of cruciferous phytoalexins on the detoxification of brassilexin by the blackleg fungus pathogenic to brown mustard. Natural Product Communications 5, 883–888.

Pedras, M.S.C., Suchy, M., 2005. Detoxification pathways of the phytoalexins brassilexin and sinalexin in *Leptosphaeria maculans*: isolation and synthesis of the elusive intermediate 3-formylindolyl-2-sulfonic acid. Organic and Biomolecular Chemistry 3, 2002–2007.

Pedras, M.S.C., Taylor, J.L., 1993. Metabolism of the phytoalexin brassinin by the 'Blackleg Fungus'. Journal Natural Products 56, 731–738.

Pedras, M.S.C., Khan, A.Q., Taylor, J.L., 1998. The phytoalexin camalexin is not metabolized by *Phoma lingam*, *Alternaria brassicae*, or phytopathogenic bacteria. Plant Science 139, 1–8.

Pedras, M.S.C., Ahiahonu, P.W.K., Hossain, M., 2004. Detoxification of the phytoalexin brassinin in *Sclerotinia sclerotiorum* requires an inducible glucosyltransferase. Phytochemistry 65, 2685–2694.

Pedras, M.S.C., Gadagi, R.S., Jha, M., Sarma-Mamillapalle, V.K., 2007a. Detoxification of the phytoalexin brassinin by isolates of *Leptosphaeria maculans* pathogenic on brown mustard involves an inducible hydrolase. Phytochemistry 68, 1572–1578.

Pedras, M.S.C., Zheng, Q.A., Sarma-Mamillapalle, V.K., 2007b. The phytoalexins from Brassicaceae: structure, biological activity, synthesis and biosynthesis. Natural Product Communications 2, 319–330.

Pedras, M.S.C., Chumala, P.B., Jin, W., Islam, M.S., Hauck, D.W., 2009. The phytopathogenic fungus *Alternaria brassicicola*: phytotoxin production and phytoalexin elicitation. Phytochemistry 70, 394–402.

Sexton, A.C., Minic, Z., Cozijnsen, A.C., Pedras, M.S.C., Howlett, B.J., 2009. Cloning, purification and characterization of brassinin glucosyltransferase, a phytoalexin-detoxifying enzyme from the plant pathogen *Sclerotinia sclerotiorum*. Fungal Genetics and Biology 46, 201–209.

Shvekhgeimer, G.A., Kelarev, V.I., Dyankova, L.A., 1984. Synthesis and properties of azoles and their derivatives: 37. Synthesis of 3,5-disubstituted 1,2,4-oxadiazoles containing indolyl radicals. Khimiya Geterotsiklicheskikh Soedinenii 12, 1609–1615.

Stefanato, F.L., Abou-Mansour, E., Buchala, A., Kretschmer, M., Mosbach, A., Hahn, M., Bochet, C.G., Métraux, J.-P., Schoonbeek, H.-J., 2009. The ABC transporter BcatrB from *Botrytis cinerea* exports camalexin and is a virulence factor on *Arabidopsis thaliana*. The Plant Journal 58, 499–510.

Williamson, B., Tudzynski, B., Tudzynski, P., Van Kan, J.A.L., 2007. *Botrytis cinerea*: the cause of grey mould disease. Molecular Plant Pathology 8, 561–580.